



# Mathematical modeling of chickenpox in Phuket: Efficacy of precautionary measures and bifurcation analysis

Sayooj Aby Jose <sup>a,c</sup>, R. Raja <sup>b,f</sup>, J. Dianavinnarasi <sup>d</sup>, D. Baleanu <sup>e,f</sup>, A. Jirawattanapanit <sup>g,\*</sup>

<sup>a</sup> Department of Mathematics, Alagappa University, Karaikudi 630 004, India

<sup>b</sup> Ramanujan centre for Higher Mathematics, Alagappa University, Karaikudi 630 004, India

<sup>c</sup> Faculty of Mathematics- Informatics Teacher Education, Dong Thap University, Viet Nam

<sup>d</sup> Center for Nonlinear Systems, Chennai Institute of Technology, Chennai 600069, Tamil Nadu, India

<sup>e</sup> Department of Mathematics, Cankaya University, Ankara 06530, Turkey

<sup>f</sup> Department of Computer Science and Mathematics, Lebanese American University, Beirut, Lebanon

<sup>g</sup> Department of Mathematics, Faculty of Science and Technology, Phuket Rajabhat University, Phuket, Thailand

## ARTICLE INFO

### Keywords:

Mathematical modeling  
Equilibrium points  
Generation matrix approach  
Bifurcation analysis  
Global asymptotic stability

## ABSTRACT

In this paper, a mathematical model depicting the transmission dynamics of Chickenpox is developed by incorporating a new parameter denoting the rate of precautionary measures. The influence and the importance of following precautionary measures are showed by applying the real data collected at Phuket province, Thailand. The model analysis such as positivity and boundedness of the solutions are provided. The rate of precaution for the spread of chickenpox was a factor that influenced the basic reproductive number, which was calculated using the next-generation matrix approach. The model's equilibrium points are identified, and the condition for the disease-free equilibrium's local and global asymptotic stability is established. The model also shows forward bifurcation. Numerical simulation is carried out to show the importance of considering the precautionary measures while controlling the disease spread and the influence of those introduced parameters are depicted graphically. Though our results, we concluded that the rate of precautionary measures plays an vital role at the same time it reduces the chance of getting infected by Chickenpox virus.

## 1. Introduction

Mathematics plays an important role in human life, it can be applied in many fields [1–8]. In particular, medical professionals can apply mathematics to simulate disease incidence and treatment and as a tool to help understand many aspects of health, such as the environment that causes various diseases and disease prevention. The significance and advantages of using mathematical models to simulate at-risk populations, infections, vectors, and infected individuals in order to address the ongoing crises of numerous diseases [9–14]. The dynamical behaviour of infectious diseases has been widely described using mathematical models. One of epidemiology's main concerns is the study of epidemic models with vaccination and treatment [15–17]. Studying the mathematical models of epidemics makes it possible to know the epidemic and the results obtained from the model. Identifying characteristics that can limit the spread of the disease can support researchers. Including having a correct understanding of the transmission of the disease. The study also identifies the strengths of a mathematical model capable of modifying epidemic characteristics. Analyzing the

model data shows its effectiveness and understanding of the epidemic's evolution and disease control measures. As a result, the findings of this study are very helpful in lowering the risk of infection, preventing the spread of infection, and controlling epidemics.

An air-borne disease named Chickenpox caused by Varicella Zoster Virus (VZV) recorded almost every countries [18]. Chickenpox is characterized by a flat red rash, blisters, bumps spreading on the face, body and back, and fever. Varicella virus, or Human herpes virus type 3, is the same virus that causes shingles. By direct contact with the blister or by touching objects such as water glasses, handkerchiefs, towels, blankets, mattresses, etc., that have been contaminated by the blister of a person with chickenpox or shingles inhaled by the blister droplets through the mucous membrane. The incubation period 10–20 days in cases of shingles can be transmitted in the form of chickenpox, especially by nursing mothers. When considering by age group, it was found that the 5–9-year-old group had the highest morbidity rate of 579 per 100,000 population, followed by the 0–4 age group, 10–14 years old and the group over 15 years old. Early chickenpox symptoms start

\* Corresponding author.

E-mail address: [anuwat.j@pkru.ac.th](mailto:anuwat.j@pkru.ac.th) (A. Jirawattanapanit).

<https://doi.org/10.1016/j.bspc.2023.104714>

Received 18 November 2022; Received in revised form 2 February 2023; Accepted 14 February 2023

Available online 24 February 2023

1746-8094/© 2023 Elsevier Ltd. All rights reserved.

with a low-grade fever in young children, but adults tend to have a high fever and blisters appear within 1–2 days. It starts from the body and face and then spreads to the arms and legs [19,20].

In history, there exist numerous number of research articles that studies the spread dynamics of Chickenpox by the aid the mathematical models. For instance, the authors of [21–23] were studied the effects of implementing vaccination strategies against VZV by developing SIR, SVEIR models. In [24], SVEITR models of Chickenpox is analyzed in the presence of control measures such as vaccinations, medical assistance for infected individuals. The authors of [25], thought about how the conventional SEIR model was used to quantitatively describe the importance of immunization of newborn infants against the chickenpox and treatment of both latently and actively infected individuals in preventing the spread of the disease. Anyways the vaccine protects up to 70 to 90 percent of people from severe illness [18]. In [26], the characteristics of a basic discrete-time stochastic model is examined. According to [17], suitable compartmentalized mathematical is proposed and analyzed the model analytically as well as numerically for its stability results. In [27], a mathematical model in both deterministic and stochastic models were examined via the Euler Maruyama method. Also, the author proved that the susceptible population increase in size when the vaccine wanes. In recent years fractional order models of VZV spread is also attracts the researchers. In [28], the author studied the detailed analysis of fractional order MSEIR model in the sense of Atangana–Baleanu (Caputo).

Various field studies of chickenpox recorded in [29–32]. Chickenpox in Phuket is a highly contagious disease. Especially in school nurseries or according to the general residential community, It is a disease that can be found all year round. Still, it tends to spread during the winter at the end of the year and at the beginning of every year [33]. Information on surveillance of chickenpox at level Thailand found that in 2016 there was a morbidity rate of 71.52 cases per 100,000 population. In 2017, there was a morbidity rate of 91.28 cases per 100,000 population. Found in the school-age group the most. Surveillance of the disease in Phuket found that in 2016 there was a sickness rate of 90.70 cases per 100,000 population, and in 2017 there was a sickness rate of 115.63 cases per 100,000 population. It is most common in the school-age group. This information reflects that chickenpox is a problem. Important public health in Phuket For this reason, the study authors saw the benefit of evaluating the chickenpox surveillance system in hospitals, schools, and other places in Phuket would allow them to know. Surveillance system performance can improve and plan for the protection and better control of the disease.

By studying a mathematical model, the chickenpox epidemic is known to spread. Moreover, complications are caused by chickenpox. This complication is often found in newborns, adults, or people with impaired immune systems. Bacterial skin infections, bloodstream infections, thrombocytopenia, pneumonia, encephalitis, and other serious consequences are the most usual and severe. The model helps the researcher to understand the factors that can control the spread of the disease. as well as having an accurate understanding of the transmission of chickenpox in Phuket. The advantage of the mathematical model is that it can modify the characteristics of the epidemic. In the data analysis process, the researcher focused on the study of patients with complications from chickenpox.

Furthermore, patients without complications will help researchers understand outbreaks' evolution and disease control measures. Therefore, the results of this study are highly beneficial in reducing the risk of chickenpox infection. Moreover, chickenpox control with the preceding, the researcher realized and saw the benefits, so they researched a mathematical model to control the chickenpox epidemic in Phuket.

The following is the paper's main contribution:

- The Mathematical model was used to investigate Chickenpox outbreaks in order to assist researchers better understand the mechanisms that control the disease's progress.

- Demonstrate the disease transmission dynamics of infected persons with and without complications.
- The local and global asymptotic stability of equilibrium points were examined through Routh Hurwitz's and Castillo-Chavez's theorems. While studying the influence of the transmission rate  $\lambda_1$ , we ended up with forward bifurcation.
- With varied levels of precautionary measures, this study would be extremely advantageous in lowering the risk of infection and reducing the basic reproductive number.

## 2. Model formulation

The study of a mathematical model demonstrates the role and utility of a mathematical model in solving the ongoing chickenpox crisis in Phuket. It simulates populations at risk of infection—pathogens, vectors, and those infected—by converting the data into mathematical equations to describe the nature of the outbreak and progression of chickenpox without the researcher needing to study directly with humans, which may endanger the lives of the researcher and the patient. It also helps to reduce the budget for supplementing measures for treatment and prevention of chickenpox in Phuket according to actual needs as quick. When numerous interacting factors are present, an infectious disease can spread in a complex manner. A mathematical model is one of the methods used to investigate and anticipate the spread and severity of a disease. This study developed a biological compartmental model that separates the human population in a Phuket city  $C$  into six compartments in order to better understand the dynamics of chickenpox. Susceptible ( $C_S$ ), Vaccinated ( $C_V$ ), Exposed ( $C_E$ ), Infected individuals with complications ( $C_{IW}$ ), Infected individuals without complications ( $C_{I\bar{W}}$ ), Recovered ( $C_R$ ) individuals are in a Phuket city  $C$ . Let  $\Lambda$  is the total recruitment. Here also we consider that susceptible individuals enter into the infected with or without complication compartment through exposed class. Susceptible people will have a rate of  $\lambda_1$  contact with infected individuals and  $\eta$  be the modification parameter that accounts for reduced transmission in infected individuals without complications. People move to vaccination class with rate of  $\lambda_2$ .  $\lambda_3$  be the waning effect, so that proportion will move to susceptible class.  $\theta$  be the vaccine efficacy, so  $(1 - \theta)$  proportion with infected and vaccinated individuals are move to exposed compartment. Disease progression rate of infectious of exposed individuals is  $\lambda_4$ . From there,  $\vartheta$  proportion move to without complicated infected compartment and remains be in complicated infected compartment.  $\psi_1$  and  $\psi_2$  are rate of recovery of infected with and without complication respectively.  $\gamma_1, \gamma_2$  and  $\gamma_3$  are natural death rate and death rate of infected with and without complication respectively. Rate of loss of infection-acquired (natural) immunity is  $\psi_3$ . The interactions and parameter descriptions are explained in Fig. 1 and summarize in Table 1. The system as follows:

$$\begin{aligned} \frac{dC_S}{dt} &= \Lambda - \lambda_1 C_S (C_{IW} + \eta C_{I\bar{W}}) + \lambda_3 C_V + \mu C_E - (\gamma + \lambda_2) C_S + \psi_3 C_R \\ \frac{dC_V}{dt} &= \lambda_2 C_S - (1 - \theta) \lambda_1 C_{IW} C_V - (1 - \theta) \lambda_1 \eta C_{I\bar{W}} C_V - (\lambda_3 + \gamma) C_V \\ \frac{dC_E}{dt} &= (1 - \theta) \lambda_1 C_{IW} C_V + (1 - \theta) \lambda_1 \eta C_{I\bar{W}} C_V + \lambda_1 C_S (C_{IW} + \eta C_{I\bar{W}}) \\ &\quad - (\lambda_4 + \gamma + \mu) C_E \\ \frac{dC_{IW}}{dt} &= \vartheta \lambda_4 C_E - (\psi_1 + \gamma + \gamma_1) C_{IW} \\ \frac{dC_{I\bar{W}}}{dt} &= (1 - \vartheta) \lambda_4 C_E - (\psi_2 + \gamma + \gamma_2) C_{I\bar{W}} \\ \frac{dC_R}{dt} &= \psi_1 C_{IW} + \psi_2 C_{I\bar{W}} - (\gamma + \psi_3) C_R \end{aligned} \quad (1)$$

where Table 1 contains a description of the parameters utilized in the aforementioned model. Model (1) presupposes that each of its variables are positive.  $C_S(0) = C_{S_0} \geq 0$ ,  $C_V(0) = C_{V_0} \geq 0$ ,  $C_E(0) = C_{E_0} \geq 0$ ,  $C_{IW}(0) = C_{I_0} \geq 0$ ,  $C_{I\bar{W}}(0) = C_{A_0} \geq 0$ ,  $C_R(0) = C_{R_0} \geq 0$ .

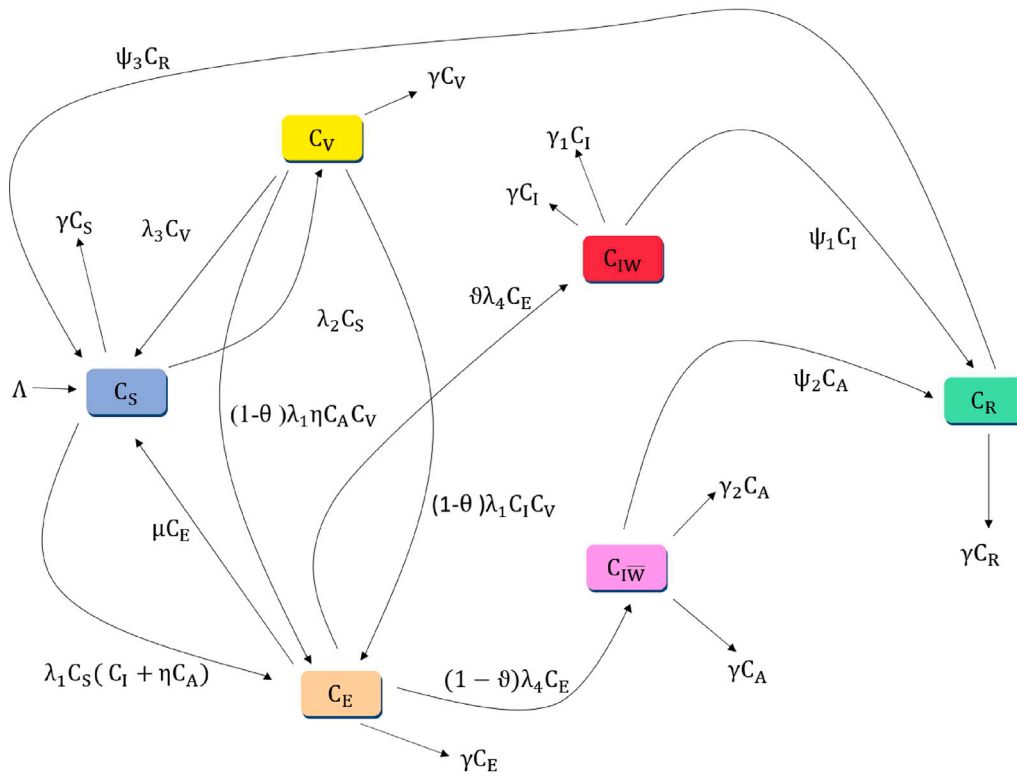


Fig. 1. Illustration for the dynamics of Chickenpox transmission.

Table 1  
Detailed description of parameters of the model (1).

Parameters	Description
$\Lambda$	Recruitment rate
$\lambda_1$	Disease transmission rate
$\eta$	Modification parameter that accounts for reduced transmission in infected individuals without complications in $C$
$\lambda_3$	Waning effect
$\lambda_2$	Vaccination rate
$\mu$	precaution taking individuals
$\theta$	Vaccine efficacy
$\lambda_4$	Disease progression rate of infectious of exposed individuals
$\vartheta$	Proportion of individuals to infected individuals with complications
$\psi_1$	The rate of recovery for those who have been infected but have complications
$\psi_2$	the rate of recovery for those who have been infected but do not have complications
$\gamma_1$	Death rate for those who have been infected and have complications
$\gamma_2$	Death rate for those who have been infected and do not have complications
$\gamma$	Natural death rate of individuals
$\psi_3$	Rate of loss of infection-acquired (natural) immunity

2.1. Analysis of the model: Basic qualitative properties

The dynamic system’s solution must be positive and bounded for all values of time  $t$  in order for the mathematical model to have biological validity. The boundedness and positivity of the solution are established by the ensuing theorem.

**Theorem 2.1 (Positivity).** Let the initial data  $C_{S_0} \geq 0, C_{V_0} \geq 0, C_{E_0} \geq 0, C_{I_0} \geq 0, C_{A_0} \geq 0, C_{R_0} \geq 0$ . Then, the solutions  $(C_S, C_V, C_E, C_{IW}, C_{IW\bar{}}, C_R)$  of model (1) are nonnegative for all  $t > 0$  in  $\mathfrak{R}_+^6$ .

**Proof.** Since it is assumed that every parameter utilized in the model is positive, the following lower bound can be determined for each equation in (1):

$$\begin{aligned} \frac{dC_S}{dt} &> -(\lambda_1(C_{IW} + \eta C_{IW\bar{}}) + (\gamma + \lambda_2))C_S, \\ \frac{dC_V}{dt} &> -((1 - \theta)\lambda_1 C_{IW} + (1 - \theta)\lambda_1 \eta C_{IW\bar{}} + (\lambda_3 + \gamma))C_V \\ \frac{dC_E}{dt} &> -(\lambda_4 + \gamma + \mu)C_E, \quad \frac{dC_{IW}}{dt} > -(\psi_1 + \gamma + \gamma_1)C_{IW} \\ \frac{dC_{IW\bar{}}}{dt} &> -(\psi_2 + \gamma + \gamma_2)C_{IW\bar{}}, \quad \frac{dC_R}{dt} > -\gamma C_R \end{aligned}$$

Solving the above inequalities respectively leads to:

$$\begin{aligned} C_S &> C_{S_0} \exp\left(-(\lambda_1 \int (C_{IW} + \eta C_{IW\bar{}}) dt + (\gamma + \lambda_2)t)\right) > 0, \\ C_V &> C_{V_0} \exp\left(-((1 - \theta)\lambda_1 \int C_{IW} dt + (1 - \theta)\lambda_1 \eta \int C_{IW\bar{}} dt + (\lambda_3 + \gamma)t)\right) > 0, \\ C_E &> C_{E_0} \exp(-(\lambda_4 + \gamma + \mu)t) > 0, \quad C_{IW} > C_{I_0} \exp(-(\psi_1 + \gamma + \gamma_1)t) > 0, \\ C_{IW\bar{}} &> C_{A_0} \exp(-(\psi_2 + \gamma + \gamma_2)t) > 0, \quad C_R > C_{R_0} \exp(-\gamma t) > 0 \end{aligned}$$

Thus, for all  $t > 0$  the solutions  $(C_S, C_V, C_E, C_{IW}, C_{IW\bar{}}, C_R)$  of model (1) are nonnegative in  $\mathfrak{R}_+^6$ .  $\square$

**Theorem 2.2 (Boundedness).** The solutions  $(C_S, C_V, C_E, C_{IW}, C_{IW\bar{}}, C_R)$  of model (1) are bounded.

**Proof.** We add each equation in the model (1) to demonstrate boundedness,  $\frac{dC_N}{dt} = \Lambda - \gamma C_N - \gamma_1 C_{IW} - \gamma_2 C_{IW\bar{}}$ , where  $C_S, C_V, C_E, C_{IW}, C_{IW\bar{}}, C_R \geq 0$ . This implies that  $\frac{dC_N}{dt}$  is bounded by  $\Lambda - \gamma C_N$ . Using standard comparison theorem [34], we obtain  $0 < C_N(t) \leq \frac{\Lambda}{\gamma}(1 - e^{-\gamma t}) + C_N(0)$ . Hence,  $\limsup_{t \rightarrow \infty} C_N(t) \leq \frac{\Lambda}{\gamma}$ .  $\square$

The model (1) is feasible in the following region  $Y = \left\{ (C_S, C_V, C_E, C_{IW}, C_{I\bar{W}}, C_R) \in \mathfrak{R}_+^6 \mid 0 \leq C_N(t) \leq \frac{A}{\gamma} \right\}$ . Also, it is the model's (1) positively invariant region. Moreover if  $C_N(0) > \frac{A}{\gamma}$  the solution of (1) either enters  $Y$  in a finite time or  $C_N(t)$  approaches  $\frac{A}{\gamma}$  asymptotically. Consequently, the region  $Y$  attracts all solutions to (1) in  $\mathfrak{R}_+^6$ .

According to the above theorem, the region  $Y$  contains all of the model's (1) feasible solutions. It is sufficient to examine the dynamics the system generates in  $Y$  because the model is said to be both mathematically and biologically well-posed [35].

2.2. Basic characteristics of the model and its local stability

In this section, we will outline the model's key characteristics before calculating its mathematical output in terms of stability analysis. We emphasize the disease free equilibrium (DFE) of model (1) given by  $\mathcal{D}_1$ , and computed as follows

$$\mathcal{D}_1 = \left( C_S, C_V, C_E, C_{IW}, C_{I\bar{W}}, C_R \right) = \left( \frac{A(\lambda_3 + \gamma)}{(\gamma + \lambda_2)(\gamma + \lambda_3) - \lambda_3\lambda_2}, \frac{\lambda_2 A}{(\gamma + \lambda_3)(\gamma + \lambda_2) - \lambda_3\lambda_2}, 0, 0, 0, 0 \right)$$

The primary factor in mathematical epidemiology that determines whether a disease may spread or be controlled is the basic reproduction number. Consequently, to derive the model's (1) basic reproduction number is denoted by  $\mathcal{R}_1$ . We apply the strategy described in [36]. The following matrices are available to us based on [36],

$$\mathcal{F} = \begin{pmatrix} 0 & \frac{\lambda_1 A [(\gamma + \lambda_3) + (1 - \theta)\lambda_2]}{(\gamma + \lambda_2)(\gamma + \lambda_3) - \lambda_3\lambda_2} & \frac{\lambda_1 \eta A [(\gamma + \lambda_3) + (1 - \theta)\lambda_2]}{(\gamma + \lambda_2)(\gamma + \lambda_3) - \lambda_3\lambda_2} \\ 0 & 0 & 0 \\ 0 & 0 & 0 \end{pmatrix}$$

$$\mathcal{V} = \begin{pmatrix} (\lambda_4 + \gamma + \mu) & 0 & 0 \\ -\vartheta\lambda_4 & (\psi_1 + \gamma + \gamma_1) & 0 \\ -(1 - \vartheta)\lambda_4 & 0 & (\psi_2 + \gamma + \gamma_2) \end{pmatrix}$$

Finally, the spectral radius of the matrix  $\rho(\mathcal{F}\mathcal{V}^{-1})$  yields the fundamental reproduction for the model (1) as

$$\mathcal{R}_1 = \left[ \frac{\lambda_1 A \vartheta \lambda_4 [(\gamma + \lambda_3) + (1 - \theta)\lambda_2]}{((\gamma + \lambda_2)(\gamma + \lambda_3) - \lambda_3\lambda_2)(\psi_1 + \gamma + \gamma_1)(\lambda_4 + \gamma + \mu)} \right] + \left[ \frac{\lambda_1 \eta A (1 - \vartheta) \lambda_4 [(\gamma + \lambda_3) + (1 - \theta)\lambda_2]}{((\gamma + \lambda_2)(\gamma + \lambda_3) - \lambda_3\lambda_2)(\psi_1 + \gamma + \gamma_2)(\lambda_4 + \gamma + \mu)} \right] = \mathcal{R}_{11} + \mathcal{R}_{12}$$

where

$$\mathcal{R}_{11} = \left[ \frac{\lambda_1 A \vartheta \lambda_4 [(\gamma + \lambda_3) + (1 - \theta)\lambda_2]}{((\gamma + \lambda_2)(\gamma + \lambda_3) - \lambda_3\lambda_2)(\psi_1 + \gamma + \gamma_1)(\lambda_4 + \gamma + \mu)} \right],$$

$$\mathcal{R}_{12} = \left[ \frac{\lambda_1 \eta A (1 - \vartheta) \lambda_4 [(\gamma + \lambda_3) + (1 - \theta)\lambda_2]}{((\gamma + \lambda_2)(\gamma + \lambda_3) - \lambda_3\lambda_2)(\psi_1 + \gamma + \gamma_2)(\lambda_4 + \gamma + \mu)} \right]$$

Next, we show the result that the model (1) at  $\mathcal{D}_1$

2.3. Local stability DFE

When the basic reproduction number  $\mathcal{R}_1 < 1$ , the dynamics of the model (1) at the disease-free scenario  $\mathcal{D}_1$  are locally asymptotically stable. We provide the outcome listed below.

**Theorem 2.3.** *The model (1) at  $\mathcal{D}_1$  is locally asymptotically stable if  $\mathcal{R}_1 < 1$ .*

**Proof.** The Jacobian matrix of the system (1) at the disease-free case  $\mathcal{D}_1$  is obtained in order to demonstrate this fact, and it is provided by (see Box 1),

It can be seen that the matrix  $J_{\mathcal{D}_1}$  has the eigenvalues,  $-(\gamma + \psi_3)$ ,  $-\gamma$ ,  $-(\lambda_2 + \lambda_3 + \gamma)$  with negative real parts. It is possible to determine the remaining four eigenvalues of the Jacobian matrix  $J_{\mathcal{D}_1}$  using the following equation:

$$\lambda^3 + \mathcal{L}_1 \lambda^2 + \mathcal{L}_2 \lambda + \mathcal{L}_3 = 0$$

$$\mathcal{L}_1 = (l_1 + l_2 + l_3), \mathcal{L}_2 = ((1 - \mathcal{R}_{11})l_1 l_2 + (1 - \mathcal{R}_{12})l_2 l_3 + l_1 l_3),$$

$$\mathcal{L}_3 = (1 - \mathcal{R}_1)l_1 l_2 l_3$$

$$l_1 = (\lambda_4 + \gamma + \mu), l_2 = (\psi_1 + \gamma + \gamma_1), l_3 = (\psi_2 + \gamma + \gamma_2)$$

Now,  $\mathcal{L}_1 \mathcal{L}_2 - \mathcal{L}_3 = (l_1 + l_2 + l_3)[(1 - \mathcal{R}_{11})l_1 l_2 + (1 - \mathcal{R}_{12})l_2 l_3] + l_1^2 l_3 + l_1 l_2^2 + \mathcal{R}_1 l_1 l_2 l_3 > 0$

Since all  $l_i > 0$ , where  $i = 1, 2, 3$ , from the above we can clearly observe that  $\mathcal{L}_i > 0$ , where  $i = 1, 2, 3$ , only if  $\mathcal{R}_1 < 1$ . Hence by Routh Hurwitz's theorem we can say that the  $\mathcal{D}_1$  is locally asymptotically stable if  $\mathcal{R}_1 < 1$ . □

**Remark 2.4.** *Theorem 2.3 indicates that an epidemic will not occur if there are only a few infected people in a population so far  $\mathcal{R}_1 < 1$ . This is true from an epidemiological perspective. It should be noted that somehow this outcome is dependent upon that population's initial infection rates. Consequently, a global stability analysis is required in order to rule out this dependency.*

2.4. Global stability of DFE

The following explores the global asymptotic stability of the model (1) for the disease-free condition  $\mathcal{D}_1$ . Using Castillo-Chavez's theorem [37], global stability analysis of DFE was investigated. Then (1),

$$\frac{dX}{dt} = F(X, Z)$$

$$\frac{dZ}{dt} = G(X, Z), \quad G(X, 0) = 0 \tag{2}$$

where  $X = (C_S, C_V, C_R) \in \mathfrak{R}^3$  denotes uninfected populations and  $Z = (C_E, C_{IW}, C_{I\bar{W}}) \in \mathfrak{R}^3$  represent the infected population.  $\mathcal{D}_1 = (X^*, 0)$  represents the DFE. If this holds the condition  $(\Theta_1), (\Theta_2)$

- $(\Theta_1)$  For  $\frac{dX}{dt} = F(X, 0)$ ,  $X^*$  is globally asymptotically stable.
- $(\Theta_2)$   $\frac{dZ}{dt} = D_Z G(X^*, 0)Z - \hat{G}(X, Z)$ ,  $\hat{G}(X, Z) \geq 0$  for all  $(X, Z) \in Y$

In light of the fact that  $\mathcal{D}_1$  is globally asymptotically stable, we draw the following conclusion, which is supported by Castillo-Chavez's theorem [37].

**Theorem 2.5.** *The equilibrium point  $\mathcal{D}_1 = (X^*, 0)$  of the system (1) is globally asymptotically stable if  $\mathcal{R}_A < 1$  and  $(\Theta_1), (\Theta_2)$  are satisfied.*

**Proof.** By defining additional variables and segmenting the system into smaller systems, we begin the proof.  $X = (C_S, C_V, C_R)$  and  $Z = (C_E, C_{IW}, C_{I\bar{W}})$ . We have two vector valued functions  $G(X, Z)$  and  $F(X, Z)$  provided by from (1),

$$F(X, Z) = \begin{pmatrix} A - \lambda_1 C_S (C_{IW} + \eta C_{I\bar{W}}) + \lambda_3 C_V + \mu C_E - (\gamma + \lambda_2) C_S + \psi_3 C_R \\ \lambda_2 C_S - (1 - \theta) \lambda_1 C_{IW} C_V - (1 - \theta) \lambda_1 \eta C_{I\bar{W}} C_V - (\lambda_3 + \gamma) C_V \\ \psi_1 C_{IW} + \psi_2 C_{I\bar{W}} - \gamma C_R - \psi_3 C_R \end{pmatrix}$$

and

$$G(X, Z) = \begin{pmatrix} (1 - \theta) \lambda_1 C_{IW} C_V + (1 - \theta) \lambda_1 \eta C_{I\bar{W}} C_V + \lambda_1 C_S (C_{IW} + \eta C_{I\bar{W}}) - (\lambda_4 + \gamma + \mu) C_E \\ \vartheta \lambda_4 C_E - (\psi_1 + \gamma + \gamma_1) C_{IW} \\ (1 - \vartheta) \lambda_4 C_E - (\psi_2 + \gamma + \gamma_2) C_{I\bar{W}} \end{pmatrix}$$

Now, let us look at the simplified system  $\frac{dX}{dt} = F(X, 0)$  from  $(\Theta_1)$

$$\frac{dC_S}{dt} = A + \lambda_3 C_V - (\gamma + \lambda_2) C_S$$

$$\frac{dC_V}{dt} = \lambda_2 C_S - (\lambda_3 + \gamma) C_V$$

$$J_{\mathcal{D}_1} = \begin{pmatrix} -(\gamma + \lambda_2) & \lambda_3 & \mu & -\lambda_1 C_{S_1} & -\lambda_1 \eta C_{S_1} & \psi_3 \\ \lambda_2 & -(\lambda_3 + \gamma) & 0 & -(1 - \theta)\lambda_1 C_{V_1} & -(1 - \theta)\lambda_1 \eta C_{V_1} & 0 \\ 0 & 0 & -(\lambda_4 + \gamma + \mu) & (1 - \theta)\lambda_1 C_{V_1} + \lambda_1 C_{S_1} & (1 - \theta)\lambda_1 \eta C_{V_1} + \lambda_1 \eta C_{S_1} & 0 \\ 0 & 0 & \vartheta \lambda_4 & -(\psi_1 + \gamma + \gamma_1) & 0 & 0 \\ 0 & 0 & (1 - \vartheta)\lambda_4 & 0 & -(\psi_2 + \gamma + \gamma_2) & 0 \\ 0 & 0 & 0 & \psi_1 & \psi_2 & -(\gamma + \psi_3) \end{pmatrix}$$

Box I.

$$D_Z G(X^*, 0) = \begin{pmatrix} -(\lambda_4 + \gamma + \mu) & (1 - \theta)\lambda_1 \frac{\lambda_2 \Lambda}{(\gamma + \lambda_3)(\gamma + \lambda_2)} + \lambda_1 \frac{\Lambda}{(\gamma + \lambda_2)} & (1 - \theta)\lambda_1 \eta \frac{\lambda_2 \Lambda}{(\gamma + \lambda_3)(\gamma + \lambda_2)} + \lambda_1 \eta \frac{\Lambda}{(\gamma + \lambda_2)} \\ \vartheta \lambda_4 & -(\psi_1 + \gamma + \gamma_1) & 0 \\ (1 - \vartheta)\lambda_4 & 0 & -\psi_2 + \gamma + \gamma_2 \end{pmatrix}$$

Box II.

$$\frac{dC_R}{dt} = 0. \tag{3}$$

We see that the dynamics of this class of infected people without complications are independent of the initial conditions in  $Y$ , implying that the convergence of the solutions of the simplified Eq. (3) is global in  $Y$ .

Then (see Box II) From  $(\Theta_2)$  we get

$$\hat{G}(X, Z) = \begin{pmatrix} A_1 \\ 0 \\ 0 \end{pmatrix},$$

where,  $A_1 = (1 - \theta)\lambda_1 \left( \frac{\lambda_2 \Lambda}{(\gamma + \lambda_3)(\gamma + \lambda_2)} - C_V \right) + \lambda_1 \left( \frac{\Lambda}{(\gamma + \lambda_2)} - C_S \right) + (1 - \theta)\lambda_1 \eta \left( \frac{\lambda_2 \Lambda}{(\gamma + \lambda_3)(\gamma + \lambda_2)} - C_V \right) + \lambda_1 \eta \left( \frac{\Lambda}{(\gamma + \lambda_2)} - C_S \right)$

Here,  $\frac{\lambda_2 \Lambda}{(\gamma + \lambda_3)(\gamma + \lambda_2)} \geq C_V, \frac{\Lambda}{(\gamma + \lambda_2)} \geq C_S$ , so we can say that  $\hat{G}(X, Z) \geq 0$  for all  $(X, Y) \in Y$ . This demonstrates that DFE is globally asymptotically stable according to LaSalle's invariance principle [38].  $\square$

### 2.5. The endemic equilibrium point

If infection persists with in the population (ie,  $C_S \geq 0, C_V \geq 0, C_E \geq 0, C_{IW} \geq 0, C_{I\bar{W}} \geq 0, C_R \geq 0$ ), the model has an equilibrium point called endemic equilibrium point represented by  $\mathcal{D}_1^*$ .

That is  $(C_S^*, C_V^*, C_E^*, C_{IW}^*, C_{I\bar{W}}^*, C_{R_1}^*) \neq 0$ . Then we obtain

$$C_S^* = \frac{k_8 - k_4 k_7 C_E^*}{k_6 + k_7 C_E^*}, C_V^* = \frac{\lambda_2 k_4}{k_6 + k_7 C_E^*}, C_{IW}^* = k_1 C_E^*,$$

$$C_{I\bar{W}}^* = k_2 C_E^*, C_R^* = k_3 C_E^*,$$

where,

$$k_1 = \frac{\vartheta \lambda_4}{(\psi_1 + \gamma + \gamma_1)}, k_2 = \frac{(1 - \vartheta)\lambda_4}{(\psi_2 + \gamma + \gamma_2)},$$

$$k_3 = \frac{\psi_1 k_1 + \psi_2 k_2}{\psi_3 + \gamma}, k_4 = \frac{(\lambda_4 + \gamma + \mu)}{\lambda_1 (k_1 + \eta k_2)},$$

$$k_5 = \frac{((1 - \theta)\lambda_1 k_1 + (1 - \theta)\lambda_1 \eta k_2)}{\lambda_1 (k_1 + \eta k_2)}, k_6 = k_5 + (\lambda_3 + \gamma),$$

$$k_7 = (1 - \theta)\lambda_1 k_1 + (1 - \theta)\lambda_1 \eta k_2,$$

$$k_8 = k_4 k_6 - k_5 \lambda_2 k_4$$

and  $C_E^*$  is the positive root of the equation  $P_1 C_{E_1}^2 + P_2 C_{E_1} + P_3 = 0$ , where,

$$P_1 = \lambda_1 k_1 k_4 k_7 + \eta k_2 k_4 k_7 + \mu k_7 + \psi_3 k_3 k_7,$$

$$P_2 = \Lambda k_7 - \lambda_1 k_1 k_8 - \eta k_2 k_8 - (\gamma + \lambda_2) k_4 k_7 + \mu k_6 + \psi_3 k_3 k_6$$

$$P_3 = \Lambda k_6 - (\gamma + \lambda_2) k_8 + \lambda_3 \lambda_2 k_4 + \mu k_6$$

### 2.6. Existence of forward bifurcation

The system's center manifold theory may be used to demonstrate the forward bifurcation occurrence (1). We conduct bifurcation analysis by applying the center manifold theorem. The following variable rearrangements and modifications must be made to the model in order to use the center manifold theory (1). Let us start by considering that,  $C_S = \varphi_1, C_V = \varphi_2, C_E = \varphi_3, C_{IW} = \varphi_4, C_{I\bar{W}} = \varphi_5, C_R = \varphi_6$ . Additionally, by employing vector notation  $C = (\varphi_1, \varphi_2, \varphi_3, \varphi_4, \varphi_5, \varphi_6)^T$  with  $\frac{dC_S}{dt} = \mathcal{L}_1, \frac{dC_V}{dt} = \mathcal{L}_2, \frac{dC_E}{dt} = \mathcal{L}_3, \frac{dC_{IW}}{dt} = \mathcal{L}_4, \frac{dC_{I\bar{W}}}{dt} = \mathcal{L}_5, \frac{dC_R}{dt} = \mathcal{L}_6, \left( \frac{dC}{dt} \right) = (\mathcal{L}_1, \mathcal{L}_2, \mathcal{L}_3, \mathcal{L}_4, \mathcal{L}_5, \mathcal{L}_6)^T$  provided in the following by choosing  $\lambda_1$  as a bifurcation parameter and solving  $\mathcal{R}_1 = 1$ , which leads to

$$\mathcal{L}_1 = \Lambda - \lambda_1 \varphi_1 (\varphi_4 + \eta \varphi_5) + \lambda_3 \varphi_2 + \mu \varphi_3 - (\gamma + \lambda_2) \varphi_1 + \psi_3 \varphi_6$$

$$\mathcal{L}_2 = \lambda_2 \varphi_1 - (1 - \theta)\lambda_1 \varphi_4 \varphi_2 - (1 - \theta)\lambda_1 \eta \varphi_5 \varphi_2 - (\lambda_3 + \gamma) \varphi_2$$

$$\mathcal{L}_3 = (1 - \theta)\lambda_1 \varphi_4 \varphi_2 + (1 - \theta)\lambda_1 \eta \varphi_5 \varphi_2 + \lambda_1 \varphi_1 (\varphi_4 + \eta \varphi_5) - (\lambda_4 + \gamma + \mu) \varphi_3$$

$$\mathcal{L}_4 = \vartheta \lambda_4 \varphi_3 - (\psi_1 + \gamma + \gamma_1)$$

$$\mathcal{L}_5 = (1 - \vartheta)\lambda_4 \varphi_3 - (\psi_2 + \gamma + \gamma_2) \varphi_5 \tag{4}$$

$$\mathcal{L}_6 = \psi_1 \varphi_4 + \psi_2 \varphi_5 - (\gamma + \psi_3) \varphi_6$$

We choose  $\lambda_1^* = \lambda_1$  as the bifurcation parameter, especially because it is more sensitive to changes in  $\lambda_1$  than any of its other parameters, in  $\mathcal{R}_1$ . If we consider  $\mathcal{R}_1 = 1$ ,

$$\lambda_1^* = \frac{((\gamma + \lambda_2)(\gamma + \lambda_3) - \lambda_2 \lambda_3)(\lambda_4 + \gamma + \mu)(\psi_1 + \gamma + \gamma_1)(\psi_1 + \gamma + \gamma_2)}{\left[ \Lambda \lambda_4 [(\gamma + \lambda_3) + (1 - \theta)\lambda_2] \right] \left[ \vartheta(\psi_1 + \gamma + \gamma_2) + \eta(1 - \vartheta)(\psi_1 + \gamma + \gamma_1) \right]} \tag{5}$$

Now, at problem DFP, the Jacobian of the linearized system (5) using the identity  $\mathcal{D}1$  when  $\lambda_1^* = \lambda_1$  is given by (see Box III), where

$$A_1 = -\lambda_1^* \frac{\Lambda}{(\gamma + \lambda_2)}, A_2 = -\lambda_1^* \eta \frac{\Lambda}{(\gamma + \lambda_2)}$$

$$J_{\mathcal{D}_1}(\lambda_1^*) = \begin{pmatrix} -(\gamma + \lambda_2) & \lambda_3 & \mu & A_1 & A_2 & \psi_3 \\ \lambda_2 & -(\lambda_3 + \gamma) & 0 & A_3 & A_4 & 0 \\ 0 & 0 & -(\lambda_4 + \gamma + \mu) & A_5 & A_6 & 0 \\ 0 & 0 & \vartheta\lambda_4 & -(\psi_1 + \gamma + \gamma_1) & 0 & 0 \\ 0 & 0 & (1 - \vartheta)\lambda_4 & 0 & -(\psi_2 + \gamma + \gamma_2) & 0 \\ 0 & 0 & 0 & \psi_1 & \psi_2 & -(\gamma + \psi_3) \end{pmatrix}$$

Box III.

$$B_1 = \frac{\lambda_2}{(\lambda_3 + \gamma)}, \quad B_2 = \frac{A_3\vartheta\lambda_4(\psi_2 + \gamma + \gamma_2) + A_4(1 - \vartheta)\lambda_4(\psi_1 + \gamma + \gamma_1)}{(\psi_2 + \gamma + \gamma_2)(\lambda_3 + \gamma)(\psi_1 + \gamma + \gamma_1)}, \quad B_3 = \frac{\vartheta\lambda_4}{(\psi_1 + \gamma + \gamma_1)},$$

$$B_4 = \frac{(B_2\lambda_3 + \mu + \psi_3 B_3)(\psi_1 + \gamma + \gamma_1)(\psi_2 + \gamma + \gamma_2) + (\psi_2 + \gamma + \gamma_2)A_1\vartheta\lambda_4 + A_2(1 - \vartheta)\lambda_4(\psi_1 + \gamma + \gamma_1)}{(\psi_2 + \gamma + \gamma_2)((\gamma + \lambda_2) - B_1\lambda_3)(\psi_1 + \gamma + \gamma_1)}$$

Box IV.

$$A_3 = -(1 - \theta)\lambda_1^* \frac{\lambda_2 A}{(\gamma + \lambda_3)(\gamma + \lambda_2)}, \quad A_4 = -(1 - \theta)\lambda_1^* \eta \frac{\lambda_2 A}{(\gamma + \lambda_3)(\gamma + \lambda_2)},$$

$$A_5 = (1 - \theta)\lambda_1^* \frac{\lambda_2 A}{(\gamma + \lambda_3)(\gamma + \lambda_2)} + \lambda_1^* \frac{A}{(\gamma + \lambda_2)},$$

$$A_6 = (1 - \theta)\lambda_1^* \eta \frac{\lambda_2 A}{(\gamma + \lambda_3)(\gamma + \lambda_2)} + \lambda_1^* \eta \frac{A}{(\gamma + \lambda_2)}$$

To compute the right eigenvector,  $\tau = (\tau_1, \tau_2, \tau_3, \tau_4, \tau_5, \tau_6)^T$ , take the system  $J\tau = 0$ .

$$\begin{aligned} -(\gamma + \lambda_2)\tau_1 + \lambda_3\tau_2 + \mu\tau_3 + A_1\tau_4 + A_2\tau_5 + \psi_3\tau_6 &= 0 \\ \lambda_2\tau_1 - (\lambda_3 + \gamma)\tau_2 + A_3\tau_4 + A_4\tau_5 &= 0 \\ -(\lambda_4 + \gamma + \mu)\tau_3 + A_5\tau_4 + A_6\tau_5 &= 0 \\ \vartheta\lambda_4\tau_3 - (\psi_1 + \gamma + \gamma_1)\tau_4 &= 0 \\ (1 - \vartheta)\lambda_4\tau_3 - (\psi_2 + \gamma + \gamma_2)\tau_5 &= 0 \\ \psi_1\tau_4 + \psi_2\tau_5 - (\gamma + \psi_3)\tau_6 &= 0 \end{aligned} \tag{6}$$

From (6) we get,

$$\begin{aligned} \tau_1 &= B_4\tau_3 \\ \tau_2 &= (B_1B_4 + B_2)\tau_3 \\ \tau_3 &= \tau_3 > 0 \\ \tau_4 &= B_3\tau_3 \\ \tau_5 &= \frac{(1 - \vartheta)\lambda_4\tau_3}{(\psi_2 + \gamma + \gamma_2)} \\ \tau_6 &= \frac{[\psi_1\vartheta\lambda_4(\psi_2 + \gamma + \gamma_2) + ((1 - \vartheta)\lambda_4\psi_2)(\psi_1 + \gamma + \gamma_1)]\tau_3}{(\psi_1 + \gamma + \gamma_1)(\gamma + \psi_3)(\psi_2 + \gamma + \gamma_2)} \end{aligned}$$

where (see Box IV)

Next, we must determine the left eigenvector,  $\tau^* = (\tau_1^*, \tau_2^*, \tau_3^*, \tau_4^*, \tau_5^*, \tau_6^*)^T$ , take the system  $\tau^*J = 0$ .

$$\begin{aligned} -(\gamma + \lambda_2)\tau_1^* - \lambda_2\tau_2^* &= 0 \\ \lambda_3\tau_1^* - (\lambda_3 + \gamma)\tau_2^* &= 0 \\ \mu\tau_1^* - (\lambda_4 + \gamma + \mu)\tau_3^* + \vartheta\lambda_4\tau_4^* + (1 - \vartheta)\lambda_4\tau_5^* &= 0 \\ A_1\tau_1^* + A_3\tau_2^* + A_5\tau_3^* - (\psi_1 + \gamma + \gamma_1)\tau_4^* + \psi_1\tau_6^* &= 0 \\ A_2\tau_1^* + A_4\tau_2^* + A_6\tau_3^* - (\psi_2 + \gamma + \gamma_2)\tau_5^* + \psi_2\tau_6^* &= 0 \\ \psi_3\tau_1^* - (\gamma + \psi_3)\tau_6^* &= 0 \end{aligned} \tag{7}$$

From (7),

$$\begin{aligned} \tau_1^* = \tau_2^* = \tau_6^* &= 0, \\ \tau_3^* = \tau_3^* &> 0, \\ \tau_4^* &= \frac{A_5}{(\psi_1 + \gamma + \gamma_1)}\tau_3^*, \quad \tau_5^* = \frac{A_6}{(\psi_2 + \gamma + \gamma_2)}\tau_3^* \end{aligned}$$

To guarantee that the eigenvector satisfies the condition  $\tau_3 \cdot \tau_3^* = 1$ , We have considered the expression for the  $\lambda_1^*$ , in which  $\tau_3^*$  is computed. The bifurcation's direction  $\mathcal{R}_C = 1$ , the direction of the bifurcation coefficients  $a$  and  $b$ , which were determined from the partial derivatives above, defines:

$$\begin{aligned} a &= -2\tau_3^2\tau_3^*\lambda_1^* \left[ B_3(B_1B_4 + B_2)(1 - \theta) + B_3B_4 \right. \\ &\quad \left. + \frac{(1 - \vartheta)\lambda_4(B_1B_4 + B_2)(1 - \theta)\eta}{(\psi_2 + \gamma + \gamma_2)} + \frac{B_4(1 - \vartheta)\lambda_4\eta}{(\psi_2 + \gamma + \gamma_2)} \right] < 0 \\ b &= \tau_3^*\tau_3 \left( \frac{A}{(\gamma + \lambda_2)} + \frac{(1 - \theta)\lambda_2 A}{(\gamma + \lambda_3)(\gamma + \lambda_2)} \right) \left( \frac{\vartheta\lambda_4}{(\psi_1 + \gamma + \gamma_1)} + \frac{\eta(1 - \vartheta)\lambda_4\tau_3}{(\psi_2 + \gamma + \gamma_2)} \right) \\ &> 0 \end{aligned} \tag{6}$$

The model experiences forward bifurcation because the sign of coefficient  $b$  is positive while that of coefficient  $a$  is negative. We therefore reach the theorem that follows

**Theorem 2.6.** At  $\mathcal{R}_C = 1$ , the model (1) indicate forward bifurcation.

### 3. Numerical simulations

To validate the findings of analytical experiments, numerical experiments are examined. The population of Phuket in 2021 is 418,785 people. Phuket Province, Thailand consists of 3 districts, Mueang Phuket, Kathu and Thalang. Mueang Phuket District has more than 300 cases of chickenpox. And Thalang has less than 300 cases of chickenpox as shown in Fig. 2.

The research results as a mathematical model for chickenpox epidemic control can be used as preliminary information on disease prevention to reduce the number of cases and to be used as academic information for surveillance agencies. With infectious diseases for children of the Epidemiology Unit, Department of Disease Control, Phuket Province, as well as presenting information to the public health authorities, taking measures to control and prevent chickenpox following various measures suitable for the general population in Phuket at risk of contracting chickenpox and reduce the number of chickenpox cases. The suggested model's experimental baseline parameters can be found in Table 1. Stability of the model (1) is investigated numerically by initial population such as (see Table 2)

- Number of Susceptible individuals: 83,812 people
- Number of Vaccinated individuals: 573 people
- Number of Exposed individuals: 604 people
- Number of Infected individuals with complications: 70 people.

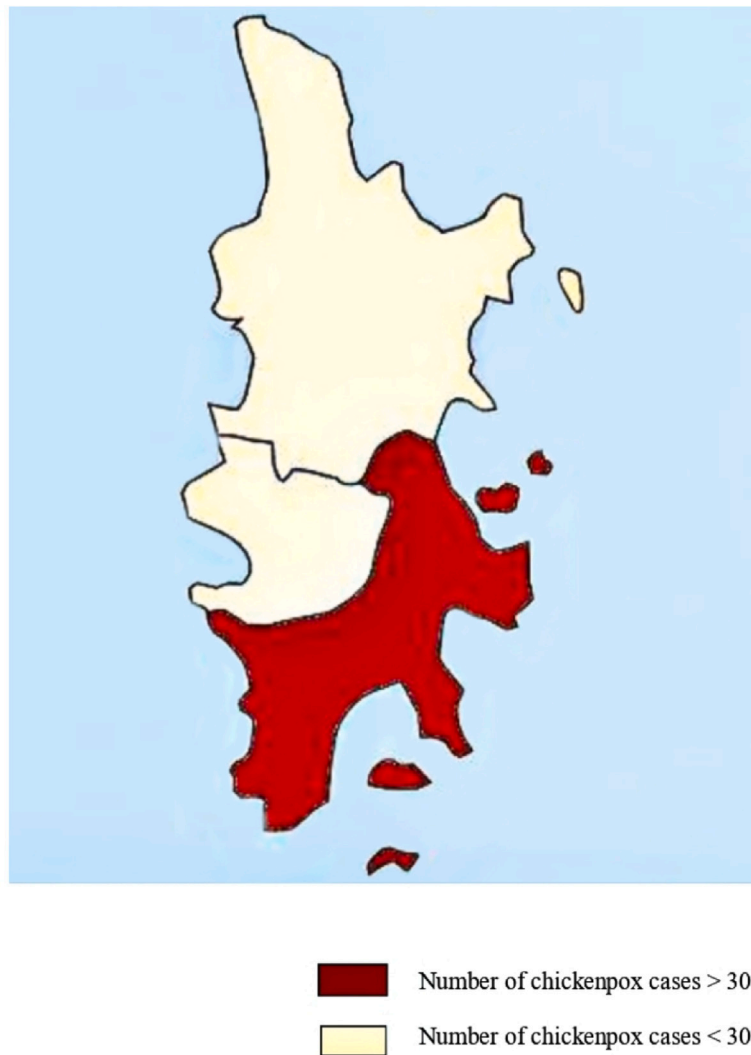


Fig. 2. Spread map of Chickenpox in Phuket province.

**Table 2**  
Defining the model's parameter values.

Variables	Value (day <sup>-1</sup> )	Source
$\Lambda$	9	[39]
$\lambda_1$	0.000010778	[39]
$\eta$	0.002218	[39]
$\lambda_3$	0.03423	Assume
$\lambda_2$	0.000504	[39]
$\mu$	0.157	Assume
$\theta$	0.0684	[39]
$\lambda_4$	0.00242	[39]
$\vartheta$	0.000318	[39]
$\psi_1$	0.000106	[39]
$\psi_2$	0.002105	[39]
$\gamma_1$	0.00001694	[39]
$\gamma_2$	0.00001694	[39]
$\gamma$	0.00001694	[39]
$\psi_3$	0.000429	[39]

**Table 3**  
Impact of  $\mu$  in  $\mathcal{R}_1$ .

Precaution ( $\mu$ )	$\mathcal{R}_1$
0.0006	16.39017
0.0012	13.68622
0.0083	4.63595
0.0342	1.35862
0.0783	0.61652
0.2383	0.20676
0.6423	0.07720
0.8123	0.06109

- Number of Infected individuals without complications: 464 people.
- Number of Recovered individuals: 178 people.

Table 3 depicts the association between  $\mathcal{R}_1$  and preventative measures. Its apparent from the table that even a slight change in  $\mu$  reflects

a significant variation in  $\mathcal{R}_1$ , that is a slight increase in  $\mu$  causes a sharp decline in  $\mathcal{R}_1$ .

Figs. 3–5 illustrates a plot which shows the dynamics of the reproduction number by varying the parameters. The plots helps to forecast reproduction number in relation to the input variables. With the use of the plot, we can understand how each parameters affect the reproduction number.

Figs. 6–11 shows the simulation of susceptible individuals, vaccinated individuals, exposed individuals, infected individuals with complications, infected individuals without complications, and recovered individuals, respectively. In Fig. 6, which represents the simulation of susceptible individuals, there is an increase till day 10 and then a decrease from day 10 to day 30. But after day 30, the simulation of

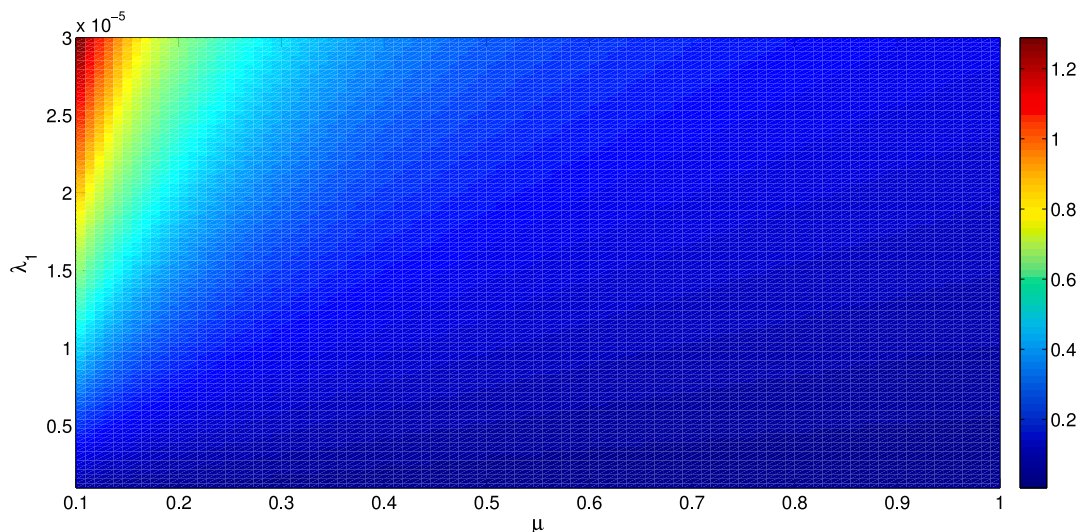


Fig. 3. The behavior of reproduction numbers ( $\mathcal{R}_1$ ) with respect to to precaution ( $\mu$ ) and Disease transmission ( $\lambda_1$ ).

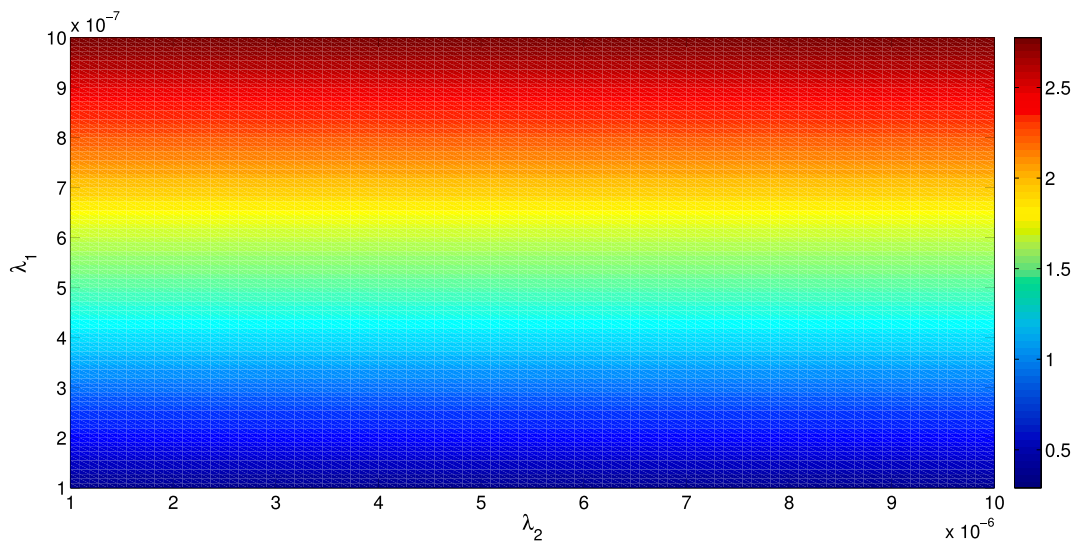


Fig. 4. The behavior of reproduction numbers ( $\mathcal{R}_1$ ) with respect to to Vaccination rate ( $\lambda_2$ ) and Disease transmission ( $\lambda_1$ ).

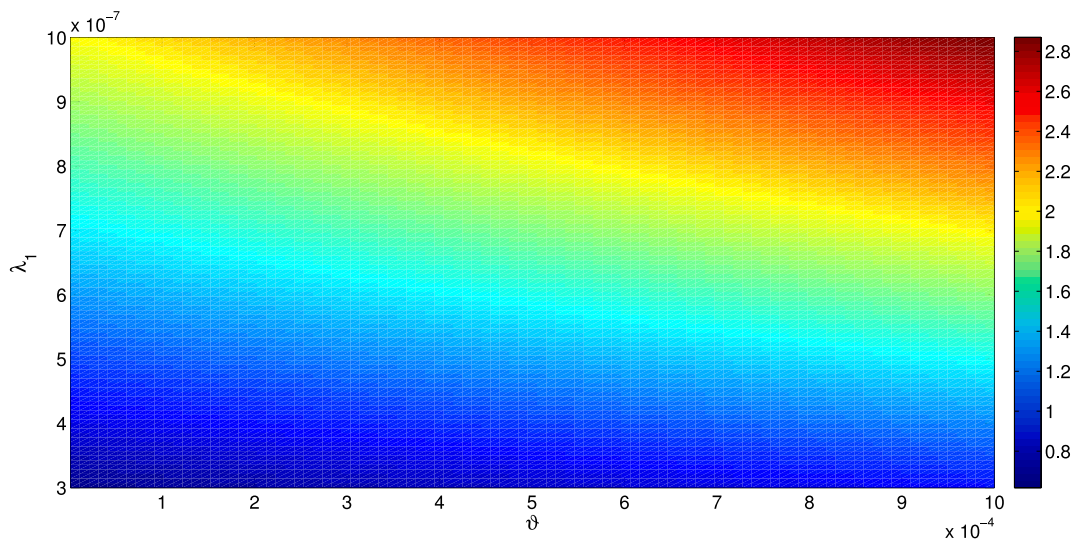


Fig. 5. The behavior of reproduction numbers ( $\mathcal{R}_1$ ) with respect to to Proportion of individuals to infected individuals with complications ( $\theta$ ) and Disease transmission ( $\lambda_1$ ).

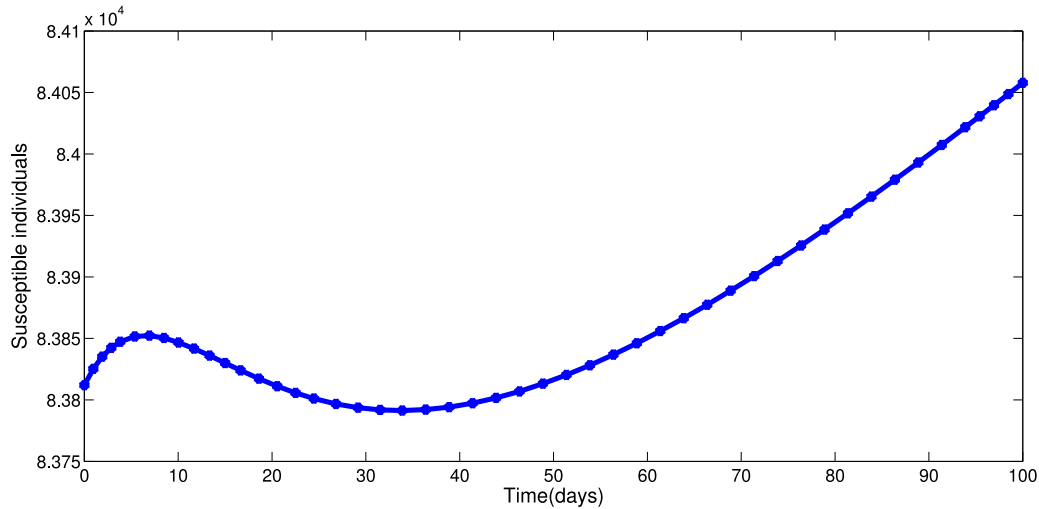


Fig. 6. Simulation of susceptible individuals.

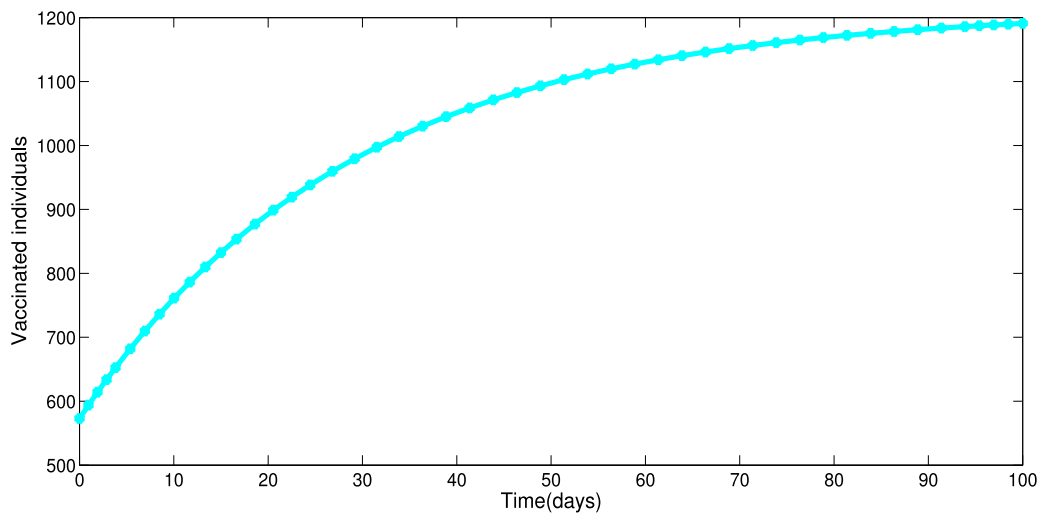


Fig. 7. Simulation of vaccinated individuals.

susceptible individuals is increased. As shown in Fig. 7, simulation is increasing gradually for vaccinated individuals. From Fig. 8 of exposed individuals, it is showing a steady decrease till day 20 and is having a constant momentum afterwards. In Fig. 9, infected individuals with complications show a steep decrease from day 1 to day 100. In Fig. 10, for infected people without complications, till day 10 there is a steady increase, but after that it is decreasing. In Fig. 11, there is a steep increase in the simulation for recovered individuals.

*Efficacy of precautionary measures on the model*

From Figs. 12–13 we can observe that when we started to follow precautionary measures there are notable decrease in the infected population. In our model (1), we considered one parameter  $\mu$  as a precautionary measure, which influence the rate of disease spread. In our simulation we tried to show that how this particular parameter used to reduce the size of the infected population. When we gradually increased the use of precautionary measures such as quarantine and individual hygiene there is a notable decrease in both infected individuals with and without complications compartments.

We are implementing the precautionary measures in an increasing manner and see how it influence the disease spread. That is, when  $\mu$

takes the values such as 0, 1%, 5%, 20%, 40%, 80%. We observe that when there is no precautionary measure ( $\mu = 0$ ), the number of infected individuals without complication is 661 and 1150 in 50 and 100 days respectively. And when we increasing the precautionary measures such as  $\mu = 1\%, 5\%, 20\%, 40\%, 80\%$ , we can notice a considerable amount of decrease in infected individuals without complication is 622&938, 533&618, 457&448, 438&412, 428&394 in 50 and 100 days respectively. From this illustration we can simply conclude that to control the spread and deaths due to chickenpox by strictly following the precautionary measures.

These total number of infected people on days 50 and 100 for various preventive measures is shown in Table 4. From Figs. 12–13 we also notice that the impact is higher in infected individuals without complication compare to infected individuals with complication while imposing preventive measures.

**Conclusion**

This research studies the mathematical model built to investigate the dynamics of chickenpox transmission with precautionary measures in Phuket province. The study results found that the factors affecting the activity of chickenpox were:

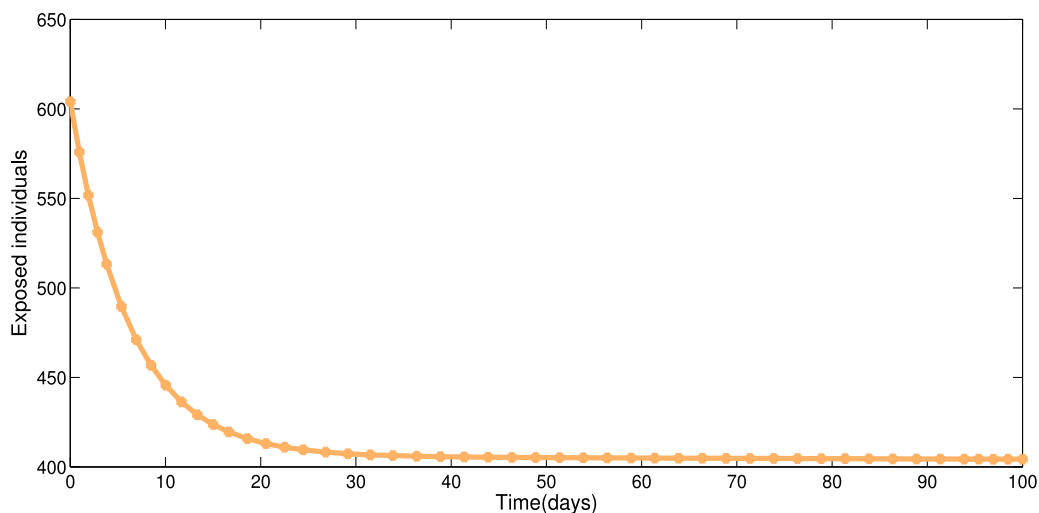


Fig. 8. Simulation of exposed individuals.

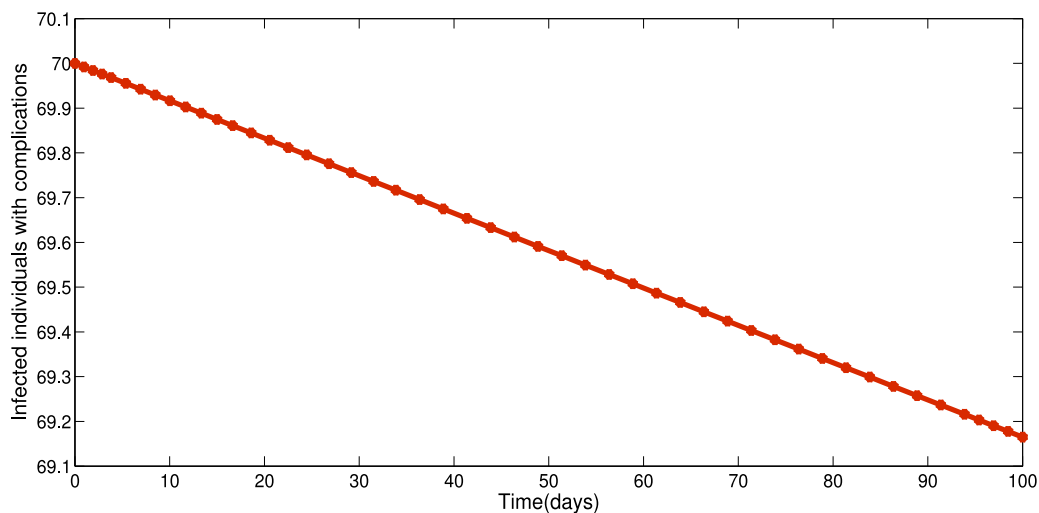


Fig. 9. Simulation of infected individuals with complications.

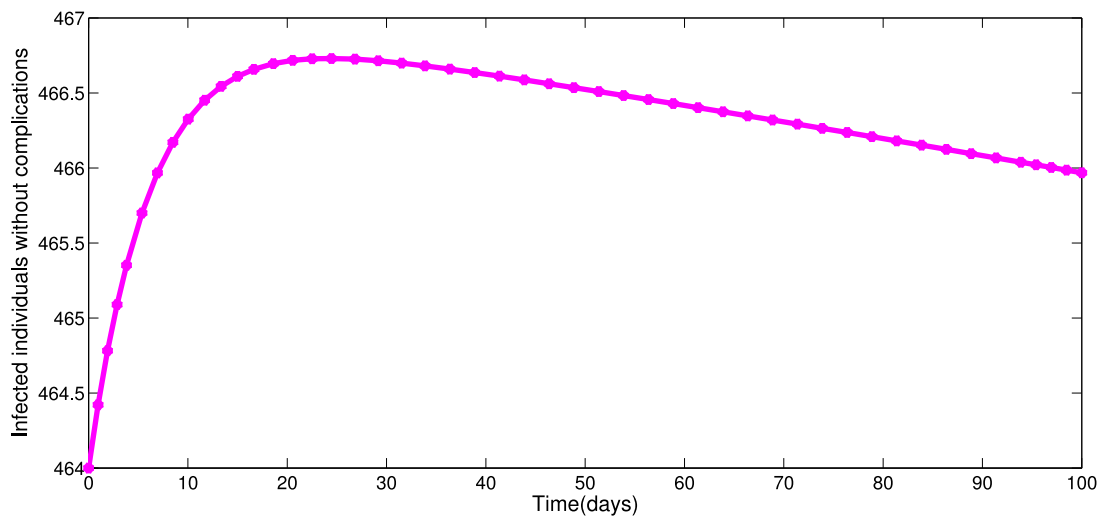


Fig. 10. Simulation of infected individuals without complications.

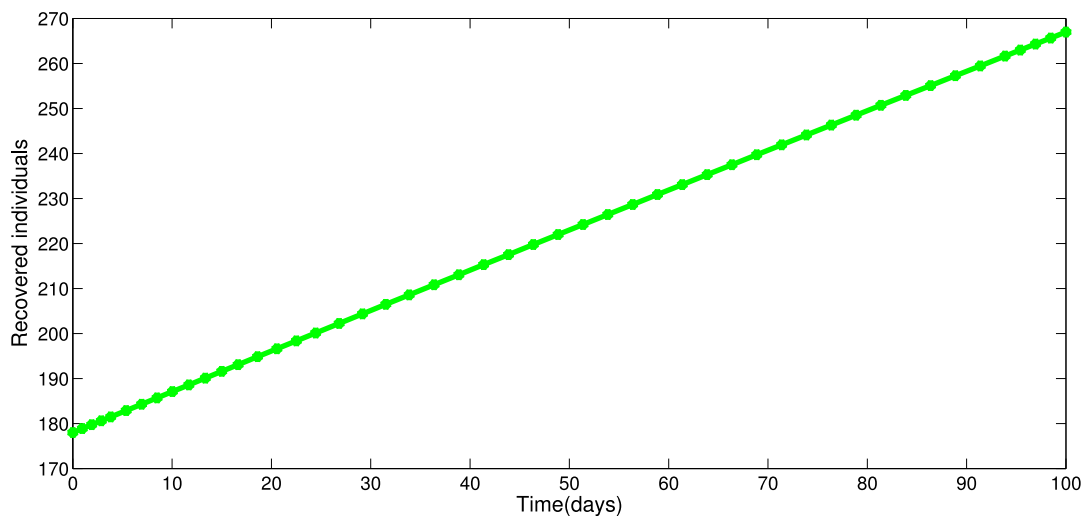


Fig. 11. Simulation of recovered individuals.

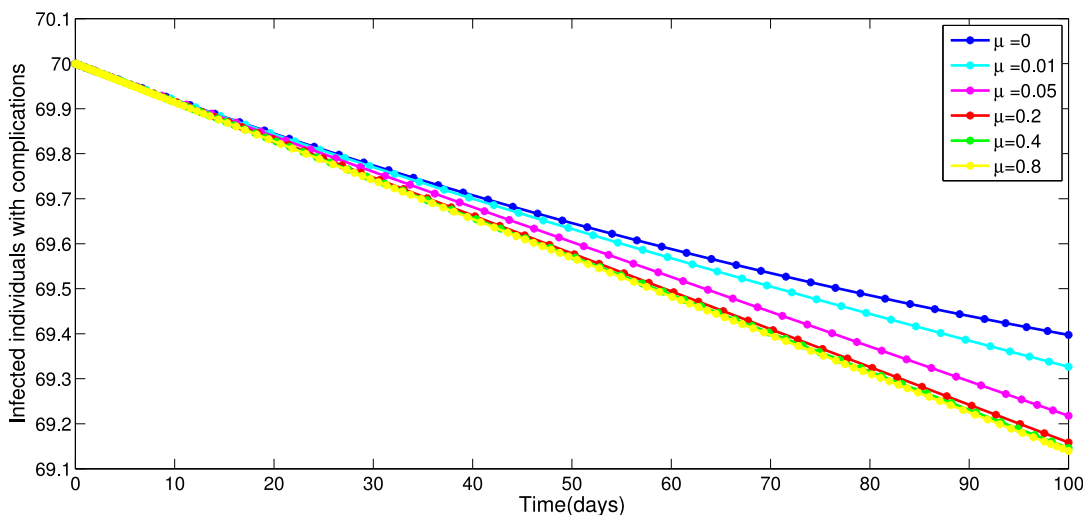


Fig. 12. Effect of precaution on Infected individuals with complications.

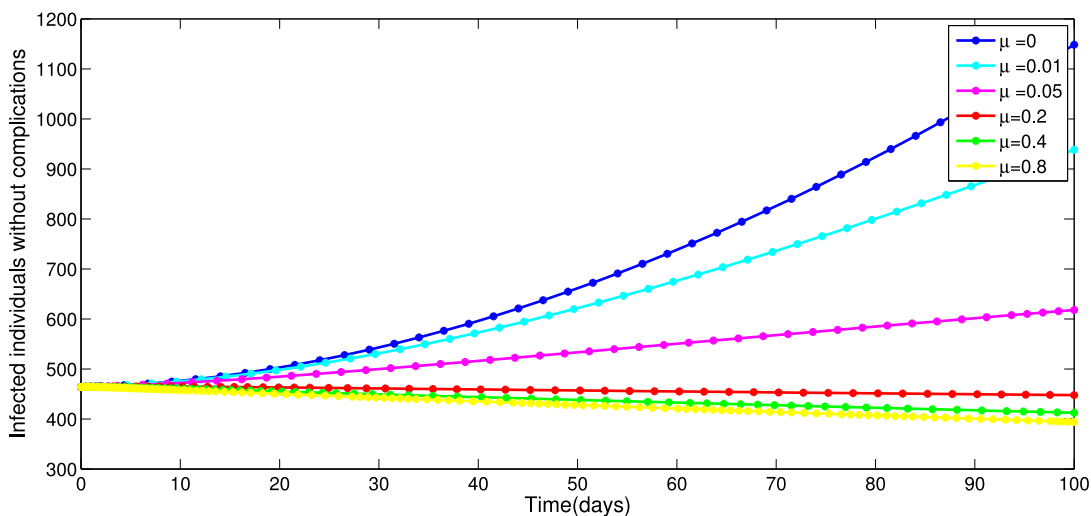


Fig. 13. Effect of precaution on Infected individuals without complications.

**Table 4**

Cumulative number of infected individuals in 50 and 100 days as varying precautionary measures.

Days	$\mu = 0$	$\mu = 0.01$	$\mu = 0.05$	$\mu = 0.2$	$\mu = 0.4$	$\mu = 0.8$
50	661	622	533	457	438	428
100	1150	938	618	448	412	394

1. The rate of a precaution for the spread of chickenpox was found to be a factor that influenced the basic reproductive number, and it was found that if the precaution was increased, the reproduction number was decreased, which meant that the precaution value would result from a reduction in the disease transmission of chickenpox in Phuket.
2. It was found that vaccination against chickenpox was directly related to the reproduction number. Therefore, an increase in the number of chickenpox vaccinations will result in lower levels of infection, which means that a large increase in the chickenpox vaccination rate will result in the spread of chickenpox decrease.
3. The factors affecting the activity of chickenpox were the number of individuals with complication group and the individuals without complication group. It was found that reducing the number of individuals with complication group to a smaller number would reduce the spread of the epidemic.

By studying efficacy of precautionary measures in mathematical model of chickenpox spread in Phuket province, the model helps the researcher to understand the factors that can control the spread of the disease, as well as having an accurate understanding of the disease transmission of chickenpox in Phuket. The advantage of the mathematical model is that it can modify the characteristics of the epidemic. Therefore, researchers understand outbreaks' evolution and disease control measures in the data analysis. Therefore, the results of this study are highly beneficial in reducing the risk of chickenpox infection. Moreover, the researcher saw the benefits of chickenpox control with the preceding, so they researched a mathematical model to control the chickenpox epidemic in Phuket.

#### Declaration of competing interest

The authors declare that they have no known competing financial interests or personal relationships that could have appeared to influence the work reported in this paper.

#### Data availability

No data was used for the research described in the article.

#### Acknowledgments

This article has been written with the joint partial financial support of IMU Breakout Graduate Fellowship Award (Ref IMU-BGF-2021-07), SERB-EQ/2019/000365, RUSA Phase II 2.0 Grant No. F 24-51/2014-U, DST (FIST—Level I) 657876570 (grant no. SR/FIST/MS-I/2018/17), Center for Nonlinear Systems, Chennai Institute of Technology, India, vide funding number CIT/CNS/2022/RP-017. Sayooj Aby Jose is thankful to FMITE, Dong Thap University for their endless support. The researcher is much obliged for the assistance provided by the Research and Development Institute. The Phuket Rajabhat University, Thailand has given immense support to this research fund. Also he would like to show his gratitude towards Phuket Provincial Public Health Office for providing vital information in support of this research.

#### References

- [1] J. Dianavinnarasi, R. Raja, J. Cao, G. Rajchakit, C.P. Lim, Global exponential stability results for the Host-Parasitoid model of sugarcane borer in stochastic environment with impulsive effects via non-fragile control: An LMI approach, *Optim. Control Appl. Methods* 43 (2) (2022) 512–531.
- [2] J. Dianavinnarasi, R. Raja, J. Alzabut, M. Niezabitowski, O. Bagdasar, Controlling Wolbachia transmission and invasion dynamics among *Aedes aegypti* population via impulsive control strategy, *Symmetry* 13 (3) (2021) 434.
- [3] J. Dianavinnarasi, R. Raja, J. Alzabut, M. Niezabitowski, G. Selvam, O. Bagdasar, An LMI approach-based mathematical model to control *Aedes aegypti* mosquitoes population via biological control, *Math. Probl. Eng.* 2021 (2021) Article ID: 5565949.
- [4] Sayooj Aby Jose, R. Raja, J. Alzabut, G. Rajchakit, Jinde Cao, Valentina E. Balas, Mathematical modeling on transmission and optimal control strategies of corruption dynamics, *Nonlinear Dynam.* (2022) <http://dx.doi.org/10.1007/s11071-022-07581-6>.
- [5] Sayooj Aby Jose, R. Raja, Quanxin Zhu, M. Niezabitowski, J. Alzabut, Valentina E. Balas, An integrated eco-epidemiological plant pest natural enemy model with different impulsive strategies, *Math. Probl. Eng.* (2022) <http://dx.doi.org/10.1155/2022/4780680>, Article ID 4780680.
- [6] Sayooj Aby Jose, R. Raja, J. Cao, J. Alzabut, M. Niezabitowski, Valentina E. Balas, Stability analysis and comparative study on different Eco-epidemiological models: Stage structure for prey and predator concerning impulsive control, *Optim. Control Appl. Methods* 43 (3) (2022) 842–866.
- [7] Sayooj Aby Jose, R. Raja, Q. Zhu, J. Alzabut, M. Niezabitowski, Valentina E. Balas, Impact of strong determination and awareness on substance addictions: A mathematical modeling approach, *Math. Methods Appl. Sci.* 45 (8) (2022) 4140–4160.
- [8] Anuwat Jirawattanapanich, Anurak Weeraprasertsakul, Sudathip Hanchongchai, Chulalak Jai-on, SEIR mathematical model for epidemic control of Chickenpox by Awareness Campaign, *Acad. J. Phuket Rajabhat Univ.* 13 (2) (2017).
- [9] P.K. Rajan, M. Kuppusamy, O.F. Egbelowo, A mathematical model for human papillomavirus and its impact on cervical cancer in India, *J. Appl. Math. Comput.* (2022) <http://dx.doi.org/10.1007/s12190-022-01767-2>.
- [10] Anip Kumar Paul, Md Abdul Kuddus, Mathematical analysis of a COVID-19 model with double dose vaccination in Bangladesh, *Results Phys.* 35 (2022) 105392.
- [11] Jayanta Kumar Ghosha, Sudhanshu Kumar Biswas, Susmita Sarkar, Uttam Ghosh, Mathematical modelling of COVID-19: A case study of Italy, *Math. Comput. Simulation* 194 (2022) 1–18.
- [12] Reetha Thomas, Sayooj Aby Jose, R. Raja, J. Alzabut, Jinde Cao, Valentina E. Balas, M. Niezabitowski, Modeling and analysis of SEIRS epidemic models using homotopy perturbation method: A special outlook to 2019-nCoV in India, *Int. J. Biomath.* (2022) <http://dx.doi.org/10.1142/S1793524522500590>.
- [13] Belela Samuel kotola, Temesgen Tibebe Mekonnen, Mathematical model analysis and numerical simulation for codynamics of meningitis and pneumonia infection with intervention, *Sci. Rep.* 12 (2022) Article number: 2639.
- [14] F.B. Agosto, S. Bewick, W.F. Fagan, Mathematical model of Zika virus with vertical transmission, *Infect. Dis. Model.* 2 (2017) 244–267.
- [15] Y. Hsieh, S. Sheu, The effect of density-dependent treatment and behaviour change on the dynamics of HIV transmission, *J. Math. Biol.* 43 (2001) 69–80.
- [16] Z. Hu, W. Ma, S. Ruan, Analysis of SIR epidemic models with nonlinear incidence rate and treatment, *Math. Biosci.* 238 (2012) 12–20.
- [17] T.J. Yusuf, F. Benyah, Optimal control of vaccination and treatment for an SIR epidemiological model, *World J. Model. Simul.* 8 (2012) 194–204.
- [18] G.P. Garnett, B.T. Greenfell, The epidemiology of Varicella-zoster virus infections: A mathematical model, *Epidemiol. Infect.* 108 (1992) 495–511.
- [19] Apichart Sivayathorn, *Dermatology Must be Known for General Medical Practice*, Village Doctor Publishing, Bangkok, 2007, 8th printing.
- [20] Chonmeth Techasaensiri, Chickenpox, Department of Pediatrics Faculty of Medicine Ramathibodi Hospital Mahidol University, Bangkok, 2021.
- [21] Donmarin, Varicella disease and varicella vaccine, 165(23), 2008, pp. 19–87.
- [22] S. Edward, D. Kuznetsor, S. Mirau, Modelling and stability analysis for a Varicella zoster virus model with vaccination, *Appl. Comput. Math.* 3 (4) (2014) 150–162.
- [23] Q.A. Ruhimat, I. Solekudin, An epidemic model of Varicella with vaccination, in: *Proceeding the 1st IBSC: Towards the Extended Use of Basic Science Health, Environment, Energy and Biotechnology for Enhancing*, ISBN: 978-602-60569-5-5.
- [24] B.C. Agbata, D. Omale, P.B. Ojih, I.U. Omatola, Mathematical analysis of Chickenpox transmission dynamics with control measures, *Cont. J. Appl. Sci.* 14 (2) (2019) 6–23.
- [25] C.N. Inyama, F.N. Mbagwu, C.M. Duru, Taxonomic relationship on some chrysophyllum species based on anatomical studies, *Med. Aromat. Plants* 5 (227) (2016) 2167–2412.
- [26] H.C. Tuckwell, R.J. Williams, Some properties of a simple stochastic epidemic model of SIR type, *Math. Biosci.* 208 (1) (2007) 76–97.
- [27] O. Bright, Osu, O. Andrew, A.I. Victory, Deterministic and stochastic models of the transmission dynamics of Chickenpox, *Nigerian Ann. Pure Appl. Sci.* 2 (2019) 185–191.

- [28] S. Qureshi, A. Yusuf, Modeling Chickenpox disease with fractional derivatives: From caputo to atangana-baleanu, *Chaos Solitons Fractals* 122 (2019) 111–118.
- [29] J. Karsai, R.C. Kovacs, A. Danielisz, Z. Molnar, J. Dudas, T. Borsos, G. Rost, Modeling the transmission dynamics of varicella in Hungary, *J. Math. Ind.* 10 (12) (2020).
- [30] U.Y. Madaki, H.A. Manu, A.A. Gwani, E.E. Elijah, Application of mathematical modelling on the spread of chickenpox disease (A case study of Nayinawa clinic damaturu, Yobe state), *Scholars J. Phys. Math. Stat.* 7 (10) (2020) 260–271.
- [31] X. Tang, S. Zhao, A.P.Y. Chiu, H. Ma, X. Xie, S. Mei, D. Kong, Y. Qin, Z. Chen, X. Wang, D. He, Modelling the transmission and control strategies of varicella among school children in Shenzhen, China, *PLoS One* 12 (5) (2017) e0177514.
- [32] J. Zibolenova, V. Szaboova, T. Baska, D. Sevcovic, H. Hudeckova, Mathematical modelling of varicella spread in slovakia, *Cent. Eur. J. Public Health* 23 (3) (2015) 227–232.
- [33] Narumon Methathien, Chickenpox, *Pediatric Infectious Disease Society of Thailand*, Bangkok, 2021.
- [34] V. Lakshmikantham, S. Leela, A.A. Martynyuk, *Stability Analysis of Nonlinear Systems*, Marcel Dekker Inc, New York, 1989.
- [35] H.W. Hethcote, *The mathematics of infectious diseases*, *SIAM Rev.* 42 (4) (2000) 599–653, <http://dx.doi.org/10.1137/S0036144500371907>.
- [36] D. Van-Driessche, J. Watmough, Reproduction numbers and subthreshold endemic equilibria for compartmental models of disease transmission, *Math. Biosci.* 180 (1) (2002) 29–48.
- [37] C. Castillo-Chavez, S. Blower, P. van den Driessche, D. Kirschner, A.A. Yakubu, *Mathematical approaches for emerging and reemerging infectious diseases: models, methods, and theory*, 1, 2002.
- [38] J.P. LaSalle, *The stability of dynamical systems*, society for industrial and applied mathematics, in: *Conference Series in Applied Mathematics*, 1976.
- [39] Phuket Provincial Public Health Office, *Phuket Health Development Strategic Plan*, Public Health Strategic Development Group, Phuket, Thailand, 2021.